Chalcogenide Letters

Tech Science Press

http://doi.org/10.32604/cl.2026.086724

ARTICLE

High Hardness $Ge_{45}As_{40}Se_{15}$ Glasses Based on Ball-Milling and Chalcogenide Glasses Molded by Spark Plasma Sintering

Jierong Gu[1,*], Licheng Hua[2], Shuangquan Xie[3,4], Xiang Shen[3,4], Tiefeng Xu[3,4] and Zijun Liu[3,4]

[1]Ningbo Institute of Oceanography, Ningbo, China
[2]Key Laboratory of Impact and Safety Engineering, Ministry of Education, Ningbo University, Ningbo, China
[3]Laboratory of Infrared Material and Devices & Key Laboratory of Photoelectric Materials and Devices of Zhejiang Province, Advanced Technology Research Institute, Ningbo University, Ningbo, China
[4]Engineering Research Center for Advanced Infrared Photoelectric Materials and Devices of Zhejiang Province, Ningbo University, Ningbo, China
*Corresponding Author: Jierong Gu. Email: gurj@nbio.org.cn

Received: 04 June 2026; Accepted: 06 July 2026; Published: 07 August 2026

ABSTRACT: In this work, $Ge_{45}As_{40}Se_{15}$ chalcogenide glass was prepared using spark plasma sintering. This method synthesizes glass powder into blocks through a certain temperature and pressure, which is an effective densification and high-precision molding of infrared transparent blocks and lenses. Through X-ray diffraction (XRD) and differential scanning calorimetry analysis, we tracked the gradual evolution of the powder during ball milling and observed the existence of a glass transition temperature in the glass after powder hot pressing. This method can prepare components outside the conventional glass forming region with high hardness and infrared transmittance, providing a simple and economical synthetic approach for preparing chalcogenide glass materials with optical application potential.

KEYWORDS: Chalcogenide glass; spark plasma sintering; glass forming region; high hardness

1 Introduction

Chalcogenide glasses are widely studied due to their unique properties, which is suitable for infrared transmission optical elements covering atmospheric windows. Chalcogenide glasses have good refractive index, thermal stability and infrared transmission [1–3]. It indicates that chalcogenide glass can serve as a potential candidate material in various fields such as infrared optical devices, optical fibers, waveguides, phase change memories, and biochemical sensors, etc. [4,5].

The common chalcogenide glasses on the current market includes As-Se, Ge-As-Se, Ge-Sb-Se and other glasses, which are usually prepared by traditional melting methods with high loss rates, even exceeding 30%. This greatly wastes raw materials and increases economic costs. Therefore, spark plasma sintering can effectively recycle and reuse the waste raw materials. In addition, the high-pressure and high-temperature environment can expand the glass forming region during this process, thus enabling the preparation of more glass that is difficult to prepare using traditional melting methods. Mathieu Hubert et al. prepared $80GeTe_2–20Ga_2Te_3$ glass outside the conventional glass forming region by combining mechanical synthesis and sintering [6–11].

At present, the hardness of chalcogenide glasses on the market is generally not high, and there is a disadvantage of being easily scratched [12–15]. The Vickers hardness of $Ge_{10}As_{40}Se_{50}$ is only 171 kgf/mm^2, the hardness of $Ge_{28}Sb_{12}Se_{60}$ is 222 kgf/mm^2 [16], the hardness of $Ge_{33}As_{12}Se_{55}$ is 251 kgf/mm^2, and the hardness of As_2Se_3 glass, which is the most commercially used chalcogenide glass in the world, is only 136 kgf/mm^2 [17]. The hardness of these commonly used chalcogenide glasses is less than 300 kgf/mm^2. Therefore, it is usually necessary to use Ge lenses as the outermost layer of lenses, but Ge materials are expensive and their performance decreases in high-temperature environments. Chalcogenide glasses based on As, Se, and Ge have a large glass forming region. Ge has a high coordination number (CN) of 4, as has a CN of 3, and Se has a CN of 2. Ge-As-Se glass can increase its mean coordination number and achieve higher hardness by adjusting the proportion of elements, which can effectively improve the problem of insufficient strength of chalcogenide glass and increase its application range [18,19].

This study is dedicated to a promising high hardness Ge-As-Se chalcogenide glass, and utilizes the highly coordinated element Ge to enhance the glass network structure. We prepared of a bulk material with a composition of $Ge_{45}As_{40}Se_{15}$ chalcogenide glass by combining mechanical synthesis and spark plasma sintering, then investigated the changes in parameters such as glass transition temperature and transmittance of the glass. In addition, XRD spectroscopy and Raman spectroscopy were used to analyze the changes in the internal structure of the glass.

2 Experimental

By employing the mechanical milling, amorphous $Ge_{45}As_{40}Se_{15}$ powder was synthesized withusing high-purity germanium (5 N), arsenic (5 N), and selenium (5 N) as raw materials. This component is outside the conventional glass-forming region, as shown in Fig. 1. The mechanical milling was performed with a planetary ball mill (Pulverisette 5 Premium, Germany). Raw materials of 5 N purity were put in a 125 mL WC bowl with 10 WC balls of a diameter of 20 mm. A ball:powder mass ratio of 10:1 was used. Rotations at 400 rpm for 30 min and 30 min pauses were alternated for several hours. The powder obtained after mechanical grinding was characterized by XRD and DSC, and then 4 g of the powder was placed in a mold with a diameter of 20 mm for sintering. The glasses were sintered by spark plasma sintering (LABOX-1575F SPS, SINTERLAND Inc., Japan). The powder ($Ge_{45}As_{40}Se_{15}$) were heated up to 770 K (50 K above T_g) under a pressure of 35 MPa for 3 min under vacuum (10^{-2} Pa).

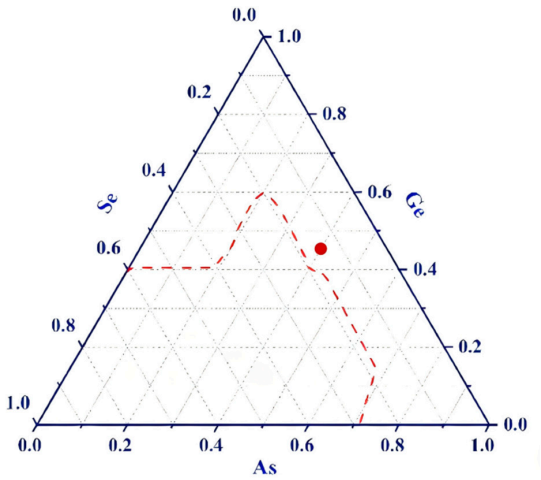

Figure 1: Glass forming domain of Ge-As-Se system [18].

Hardness was determined using a Vickers hardness tester (MH-30, Hengyi Co., China) on an average of 10 measures, with a charge of 50 g for 5 s. FTIR spectra were obtained using Nicolet 380 FTIR from 2.5 μm to 25 μm. Utilizing the D2 Phaser diffractometer manufactured by Bruker (Germany), X-ray diffraction (XRD) patterns were recorded employing CuKα radiation with a step increment of 0.016°, and the test range was from 10° to 70°. The microscopic morphology of the sample was investigated utilizing scanning electron microscopy (SEM, Tescan VEGA 3 SBH). Thermal analysis was measured by a differential scanning calorimeter (DSC, TAQ2000, USA) by heating in a sealed aluminum pan at a rate of 10°C/min under N_2 atmosphere to obtain glass transition temperature T_g, sample mass was 10 mg, test temperature is from 323 K to 850 K. All the measurements were performed at room temperature.

3 Results and Discussion

3.1 Amorphous Nature Analysis

The X-ray diffraction (XRD) pattern of the $Ge_{45}As_{40}Se_{15}$ glass is presented in Fig. 2, XRD can observe whether there is crystallization in the sample to a certain extent [20]. As shown in Fig. 2a, the XRD patterns of powders obtained at different ball milling times are presented. Multiple sharp diffraction peaks can be observed in the XRD patterns of powders with milling durations of 8, 16, and 32 h, respectively. This diffraction peak belongs to the Ge crystal phase and comes from the raw material of crystalline Ge. When the milling time reaches 48 h, the diffraction peak of the XRD is relatively weak. When the milling time is extended to 64 h, the diffraction peak of crystalline Ge disappears, indicating that the ground powder has transformed into an amorphous state. When the milling time is 80 h and 96 h, the XRD curve still does not show any diffraction peaks. Subsequently, the powders with milling times of 64 h, 80 h, and 96 h are compressed and sintered using SPS equipment, and the obtained glasses are subjected to XRD testing, as shown in Fig. 2b, and no diffraction peaks were observed in the XRD curves.

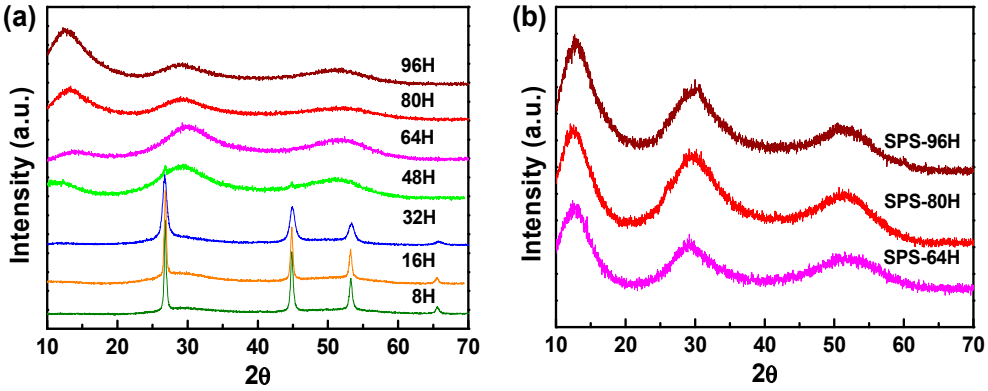

Figure 2: (**a**) The XRD curves of the powders with various milling duration of 8–96 h, (**b**) XRD curves of SPS-64h, SPS-80h and SPS-96h glass samples.

3.2 Surface Morphology Analysis

To further confirm whether microcrystals exist in the glass samples, the micro-morphology was obtained using SEM. The scanning electron microscope surface map of SPS-64h glass, SPS-80h glass and SPS-96h glass are observed in Fig. 3. It can be seen that these glass surfaces have no obvious microcrystals. However, it was also observed that as the milling time increased, more pores appeared in the glass. This is because during the milling process, there is a steady state time for the powder particles. Within the steady state time, as the ball milling time increases, the particle size of the powder decreases and the density of the

sintered glass also increases. However, beyond the steady state time, pores appear, which in turn reduces the density of the sintered glass.

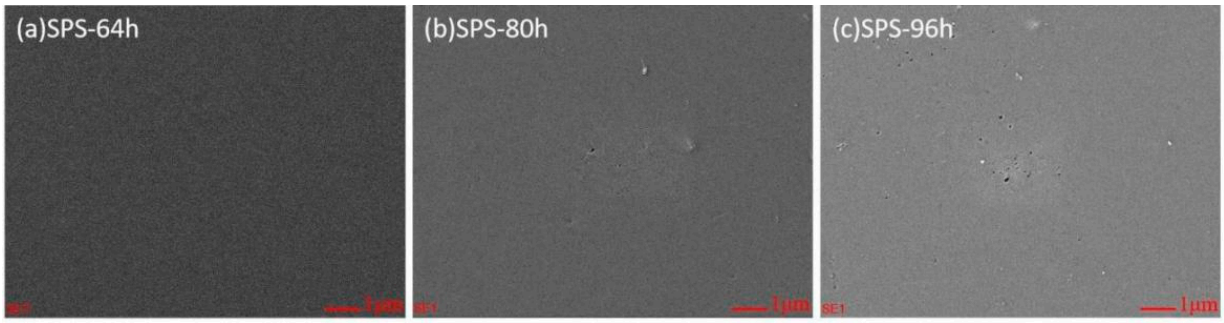

Figure 3: SEM images of (**a**) SPS-64h, (**b**) SPS-80h, (**c**) SPS-96h.

3.3 Thermal Properties Analysis

Fig. 4 shows typical DSC curves of glass samples. It can be observed that the transition temperatures and crystallization temperatures of SPS-64h glass, SPS-80h glass and SPS-96h glass are essentially identical. It can be observed that the particle size of the powder does not affect the transition temperature and crystallization temperature of the glass formed by hot pressing. Moreover, the transition temperature of the $Ge_{45}As_{40}Se_{15}$ glass is as high as 717.9 K, whereas the transition temperature of the commonly used As_2Se_3 glass is only 455 K.

Mean coordination number (MCN) can be used to describe the internal structure of glass network, and the formula is:

$$MCN = \sum_i f_i CN_i \tag{1}$$

where f_i is element's atomic fraction, CN_i is coordination number. Therefore, the *MCN* of $Ge_{45}As_{40}Se_{15}$ glass is 3.3, and the *MCN* of As_2Se_3 glass is 2.4. The glass with a larger *MCN* typically has a higher glass transition temperature and greater hardness. Since there is a positive correlation between the hardness of glass and its transition temperature, the hardness of this glass is significantly higher than that of As_2Se_3 glass. After actual testing, it was found that the Vickers hardness of the $Ge_{45}As_{40}Se_{15}$ glass was 351.1 kgf/mm^2, while the Vickers hardness of the As_2Se_3 glass was only 136 kgf/mm^2.

3.4 IR Spectra Analysis

The IR transmission spectra of SPS-64h glass, SPS-80h glass and SPS-96h glass samples are shown in Fig. 5. Although the raw material configuration is completed in a vacuum glove box, the glass sample still has a relatively large absorption peak due to the long grinding time, during which air enters the WC bowl. The absorption peak at the wavelength of 6–9 μm is As-O and Ge-O. The absorption peak at the wavelength of 9–15 μm is As-O, Se-O and Ge-O [21]. It can be observed that as the grinding time increases, the transmittance gradually decreases, with SPS-64h glass having the highest transmittance among the three samples, reaching 51%. Impurities and pores are important factors affecting the transmittance of glass. As the ball milling time increases, the powder becomes finer, resulting in an increase in internal pores in the glass, which is the main factor leading to a decrease in glass transmittance.

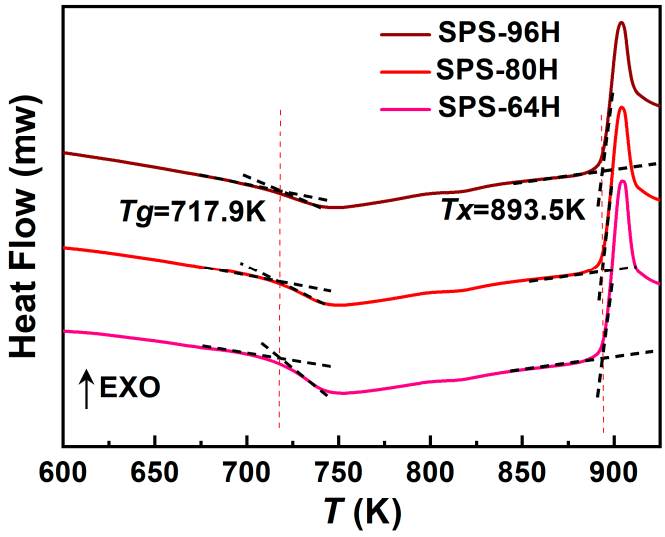

Figure 4: The DSC thermal tracking curves of SPS-64h, SPS-80h and SPS-96h glass samples.

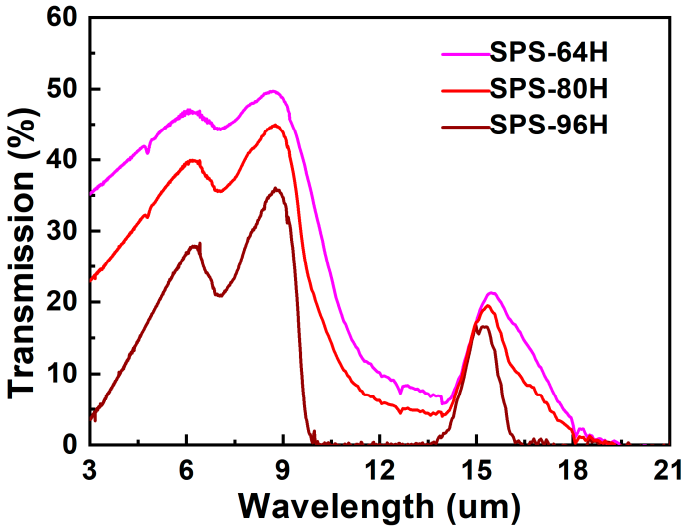

Figure 5: IR transmission spectra of SPS-64h, SPS-80h and SPS-96h glass samples.

3.5 Raman Analysis

The typical Raman spectra of the glasses are shown in Fig. 6. The strongest band at 225 cm^{-1} in As_2Se_3 spectra, is ascribed to $AsSe_{3/2}$ pyramidal units. As can be seen, with the increase of Ge content, the peak at 225 cm^{-1} disappears. This is because the Ge-Se bonding strength is 49.42 kcal/mol, while the As-Se bonding strength is only 41.69 kcal/mol. The strongest band at 190 cm^{-1} is ascribed to Ge-Se vibrations in [$GeSe_4$] tetrahedrons. The strongest band at 175 cm^{-1} is ascribed to Ge-Ge vibrations in [Se_3Ge-$GeSe_3$] structural units [22–24]. From Fig. 7, it can be observed that as the Ge content further increases, the number of Ge-Ge homopolar bonds increases, resulting in a stronger peak at 175 cm^{-1}.

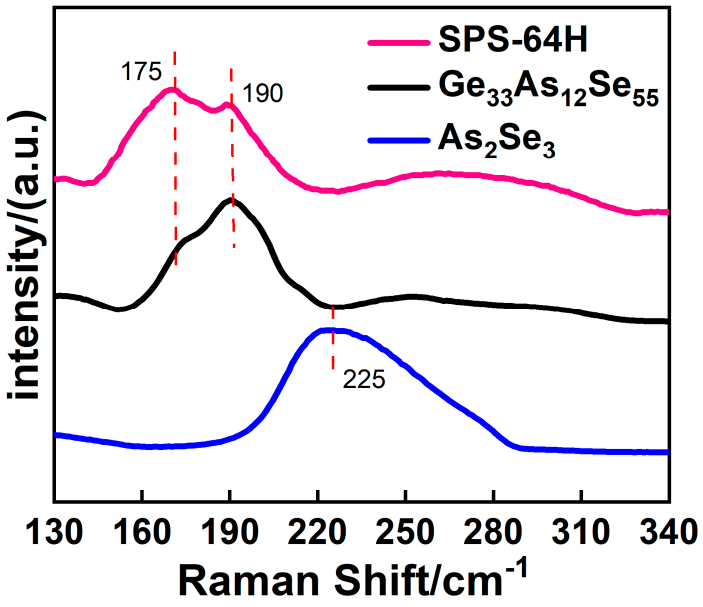

Figure 6: Raman spectra of the SPS-64h, $Ge_{33}As_{12}Se_{55}$ and As_2Se_3 glass samples.

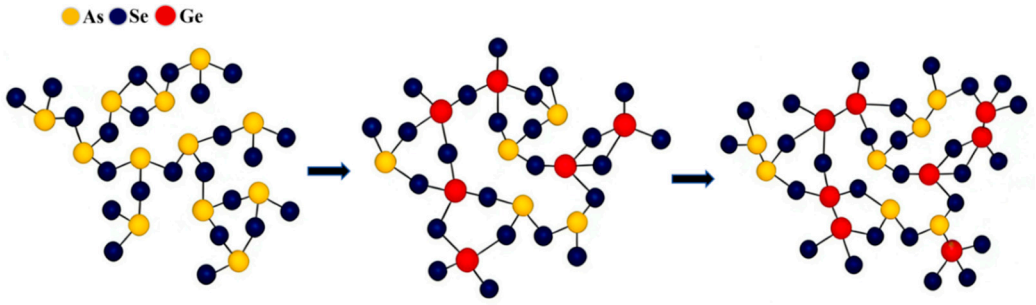

Figure 7: Schematic diagram of how Ge addition crosslinks As-Se structure.

4 Conclusions

In this study, we successfully prepared bulk $Ge_{45}As_{40}Se_{15}$ chalcogenide glass outside the conventional glass forming region using mechanical alloying method and spark plasma sintering. After 64 h of ball milling, the powder was completely vitrified, and the glass prepared by SPS had a maximum infrared transmittance of 51% and a Vickers hardness of 351.1 kgf/mm^2. As the ball milling time further increases, the glass properties degrade, so choosing a suitable ball milling time is important. The simple and economical technique of mechanical synthesis combined with spark plasma sintering proposed in this study has opened up a new way to prepare chalcogenide glass components that cannot be prepared by traditional melting/quenching methods.

Acknowledgement: The authors would like to thank Guang Jia, Yimin Chen, and Kelun Xia for their valuable advice and support.

Funding Statement: This work is supported by the National Natural Science Foundation of China (Grant No. 62075110), the Key R&D program of Zhejiang Province, China (Grant No. 2021C01025), the project of Key Laboratory of Impact and Safety Engineering, Ministry of Education (Ningbo University, CJ202506), and Joint Funds of the National Natural Science Foundation of China (U21A2056).

Author Contributions: The authors confirm contribution to the paper as follows: conceptualization, Xiang Shen; sample preparation, Jierong Gu; investigation and device design, Tiefeng Xu; XRD analysis and Raman analysis, Zijun Liu; DSC analysis, Licheng Hua; optical measurements, Shuangquan Xie. All authors reviewed and approved the final version of the manuscript.

Availability of Data and Materials: The data supporting the findings of this study are available from the corresponding author upon reasonable request.

Ethics Approval: Not applicable.

Conflicts of Interest: The authors declare no conflicts of interest.

References

1. Cha DUH, Kim HJ, Hwang Y, Jeong JC, Kim JH. Fabrication of molded chalcogenide-glass lens for thermal imaging applications. Appl Opt. 2012;51(23):5649–56. [CrossRef].
2. Fan B, Xue B, Luo Z, Zhang X, Ma H, Calvez L. Pressure dependence of interfacial resistance in pellets made from GeS_2–Ga_2S_3–Li_2S–LiI glass powder. J Am Ceram Soc. 2019;102(3):1122–7. [CrossRef].
3. He Y, Wang X, Nie Q, Xu Y, Wang G, Xu T, et al. Optical properties of Ge–Te–Ga doping Al and $AlCl_3$ far infrared transmitting chalcogenide glasses. Infrared Phys Technol. 2013;58:1–4. [CrossRef].
4. Baudrier-Raybaut M, Haïdar R, Kupecek P, Lemasson P, Rosencher E. Random quasi-phase-matching in bulk polycrystalline isotropic nonlinear materials. Nature. 2004;432(7015):374–6. [CrossRef].
5. Houizot P, Boussard-Plédel C, Faber AJ, Cheng LK, Bureau B, Van Nijnatten PA, et al. Infrared single mode chalcogenide glass fiber for space. Opt Express. 2007;15(19):12529. [CrossRef].
6. Hubert M, Petracovschi E, Zhang XH, Calvez L. Synthesis of germanium–gallium–tellurium (Ge–Ga–Te) ceramics by ball-milling and sintering. J Am Ceram Soc. 2013;96(5):1444–9. [CrossRef].
7. Premović M, Du Y, Minić D, Zhang C, Manasijević D, Balanović L, et al. Experimental investigation and thermodynamic calculation of the Cu-Ge-Sb system. J Alloys Compd. 2017;726:820–32. [CrossRef].
8. Wang J, Liu YJ, Tang CY, Liu LB, Zhou HY, Jin ZP. Thermodynamic description of the Au–Ag–Ge ternary system. Thermochim Acta. 2011;512(1–2):240–6. [CrossRef].
9. Rozé M, Calvez L, Ledemi Y, Allix M, Matzen G, Zhang XH. Optical and mechanical properties of glasses and glass–ceramics based on the Ge–Ga–Se system. J Am Ceram Soc. 2008;91(11):3566–70. [CrossRef].
10. Hubert M, Delaizir G, Monnier J, Godart C, Ma HL, Zhang XH, et al. An innovative approach to develop highly performant chalcogenide glasses and glass-ceramics transparent in the infrared range. Opt Express. 2011;19(23):23513–22. [CrossRef].
11. Suryanarayana C. Mechanical alloying and milling. Prog Mater Sci. 2001;46(1–2):1–184. [CrossRef].
12. Zhang XH, Guimond Y, Bellec Y. Production of complex chalcogenide glass optics by molding for thermal imaging. J Non Cryst Solids. 2003;326–327:519–23. [CrossRef].
13. Guin JP, Rouxel T, Sanglebœuf JC, Melscoët I, Lucas J. Hardness, toughness, and scratchability of germanium–selenium chalcogenide glasses. J Am Ceram Soc. 2002;85:1545–52. [CrossRef].
14. Michels BD, Frischat GH. Microhardness of chalcogenide glasses of the system Se-Ge-As. J Mater Sci. 1982;17:329–34. [CrossRef].
15. Yang X, Zhang M, Yan K, Han L, Xu Q, Liu H, et al. Controllable formation of the crystalline phases in Ge–Ga–S chalcogenide glass-ceramics. J Am Ceram Soc. 2017;100(1):74–80. [CrossRef].
16. Bavafa P, Rezvani M. Investigation of gallium and tin on IG5 commercial chalcogenide glass and glass ceramics. Infrared Phys Technol. 2023;128:104464. [CrossRef].
17. Sharma R, Welch RS, Kang M, Goncalves C, Blanco C, Buff A, et al. Impact of morphology and microstructure on the mechanical properties of Ge–as-Pb-Se glass ceramics. Appl Sci. 2020;10(8):2836. [CrossRef].
18. Qiu Z, Dai S, Liu C, Wu W, Xu Z, Wang Y, et al. Novel Ge-as-Se chalcogenide glass for potential high Brillouin gain coefficient of fiber. Ceram Int. 2023;49(10):16433–9. [CrossRef].
19. Xie S, Gu J, Jia G, Liu Z, Gu C, Gao Y, et al. Obtaining ultra-high hardness in spark plasma sintered $Ge_{40}As_{40}Se_{20}$ bulk glass. Infrared Phys Technol. 2024;140:105380. [CrossRef].

20. Biswas D, Gautam RKS, Singh LS, Patra AS, Mittal V, Dutta P. Effects of te substitution on optical and dielectric properties of Te–As–Ge-Se chalcogenide glasses. Appl Phys A. 2026;132:595. [CrossRef].
21. Ding S, Dai S, Cao Z, Liu C, Wu J. Composition dependence of the physical and acousto-optic properties of transparent Ge–As–S chalcogenide glasses. Opt Mater. 2020;108:110175. [CrossRef].
22. Wang RP, Smith A, Prasad A, Choi DY, Luther-Davies B. Raman spectra of $Ge_xAs_ySe_{1-x-y}$ glasses. J Appl Phys. 2009;106(4):043520. [CrossRef].
23. Zha C, Wang R, Smith A, Prasad A, Jarvis RA, Luther-Davies B. Optical properties and structural correlations of GeAsSe chalcogenide glasses. J Mater Sci Mater Electron. 2007;18(1):389–92. [CrossRef].
24. Tostanoski N, Heilweil E, Wachtel P, Musgraves J, Sundaram S. Structure-terahertz property relationship and femtosecond laser irradiation effects in chalcogenide glasses. J Non Cryst Solids. 2023;600:122020. [CrossRef].